

CLIMATE IMPACT RESPONSE FUNCTIONS AS IMPACT TOOLS IN THE TOLERABLE WINDOWS APPROACH

H.-M. FÜSSEL and F. L. TOTH*

*Potsdam Institute for Climate Impact Research, Telegrafenberg, D-14473 Potsdam, Germany
E-mail: fuessel@pik-potsdam.de*

JELLE G. VAN MINNEN

*National Institute of Public Health and the Environment, Department for Environmental
Assessment, Box 1, 3720 BA Bilthoven, The Netherlands*

FRANK KASPAR

Max Planck Institute for Meteorology, Bundesstraße 55, D-20146 Hamburg, Germany

Abstract. A critical issue for policymakers in defining mitigation strategies for climate change is the availability of appropriate evaluation tools. The development of climate impact response functions (CIRFs) is our reaction to this challenge. CIRFs depict the response of selected climate-sensitive impact sectors across a wide range of plausible futures. They consist of a limited number of climate-change-related dimensions and sensitivities of sector-specific impact models. The concept of CIRFs is defined and the procedure to develop them is presented. The use of climate change scenarios derived from various GCM experiments and the adopted impact assessment models are explained. The CIRFs presented here consider climate change impacts on natural vegetation, crop production, and water availability. They are part of the ICLIPS integrated assessment framework based on the tolerable windows approach. CIRFs can be applied both in 'forward' and in 'inverse' mode. In the latter, they help to translate thresholds for climate impacts perceived by stakeholders (so-called impact guardrails) into constraints for climate variables (so-called climate windows). This enables the results of detailed impact models to be incorporated into intertemporally optimizing integrated assessment models, such as the ICLIPS model.

Keywords: climate impact response function, tolerable windows approach, integrated assessment model, ICLIPS model, SRES scenarios

Abbreviations: AGMT – annual global mean temperature; AOGCM – coupled atmosphere-ocean general circulation model; CIRF – climate impact response function; GCM – general circulation model; ICLIPS – Integrated Assessment of Climate Protection Strategies; SRES – Special report on emissions scenarios; TWA – Tolerable Windows Approach

1. Introduction

Various approaches have been pursued to represent aggregated impacts in integrated assessment models of climate change. Models for optimal emission control based on a cost-benefit framework require monetary climate change damage functions. Early examples include DICE (Nordhaus, 1994) in which

* Present affiliation: International Institute for Applied Systems Analysis (IIASA), Schlossplatz 1, A-2361 Laxenburg, Austria



Climatic Change 00: 1–28, 2002.

© 2002 Kluwer Academic Publishers. Printed in the Netherlands.

the change in annual global mean temperature (AGMT) is the only predictor for the impacts of climate change, and FUND (Tol, 1996) which also considers the rate of change. The empirical foundation of such damage functions is, however, rather weak. The functional relationship between climate indicators and (market) impacts is typically devised by the authors and is fit to a limited number of impact assessments, e. g., current conditions and increased greenhouse gas concentrations with a radiative forcing equivalent to a doubling of CO₂ relative to its preindustrial level. Another attempt to construct 'climate-response functions' with a broader empirical base is the development of a so-called 'global impact model' (GIM; Mendelsohn et al., 2000). Here, empirical studies of the US economy are used to establish a relationship between annually averaged temperature and precipitation on the one hand and market impacts for each climate-sensitive sector on the other, which is then applied worldwide.

Recent efforts to improve the estimation of climate change impacts are also associated with integrated assessment models. For the new version of the RICE model, Nordhaus and Boyer (2000) develop a set of regionally and sectorally disaggregated impact assessments based on a willingness to pay approach. This represents a conceptual shift by recognizing that "it is the risks that are the major cause of concern about future climate change" (p. 71) and one needs to estimate the willingness to pay of different societies to avoid undesirable impacts of climate change. The estimation is undertaken for thirteen world regions and seven impact categories, including, for the first time, "catastrophic impacts" associated with major geophysical calamities. The resulting impact functions indicate the fractions of annual income that a region is willing to pay to avoid the effects of incremental climate change for a given sector.

Tol (1999a, 1999b) estimates a series of impact functions based on globally comprehensive and internally consistent studies by using GCM scenarios and develops an impact model to take account of the dynamics of both climate change and the impact sectors. The model uses statistical methods to combine and extrapolate results of different studies over different climates and different degrees of vulnerability to climate change.

Both Nordhaus and Tol express impacts as a function of temperature increase and both assume future socioeconomic vulnerability declining as a function of increasing incomes, while Tol also considers other, sector-dependent vulnerability measures. Both studies result in aggregated monetary estimates of climate change impacts. In contrast, the impact estimates presented in this paper are expressed in biophysical units, allow aggregation at different national or regional levels, avoid the intricacies of monetization and discounting, and let the users assess the socioeconomic risks associated with the biophysical effects of incremental climate change.

This paper presents a different approach to incorporating climate change impacts into an integrated assessment framework. It presents the concept of

climate impact response functions (CIRFs) and the procedures for producing them for three impacts sectors. Selected results illustrate the applicability of CIRFs in the ICLIPS (Integrated Assessment of Climate Protection Strategies) framework.

2. Method

This section starts with an introduction to the concept of CIRFs and their possible applications. Subsequently, we discuss the climate input to the CIRFs presented in this paper. Finally, the sectoral impact models that were applied in the computation of the CIRFs are described.

2.1. CIRFs: GENERAL CONCEPTS

The integrated ICLIPS model is applied in the framework of the tolerable windows approach (TWA; see Petschel-Held et al., 1999; Bruckner et al., 2003a; Toth et al., 2003). The basic idea of this decision-making framework for climate policy formulation is to separate normative judgments from scientific analysis as far as possible. In the first step of a TWA application, decision makers are asked to specify perceived limits to potential climate impacts (so-called impact guardrails) as well as requirements for an acceptable socioeconomic development. In the second step, the whole set of emission reduction strategies that simultaneously obey these constraints are identified by a model-based analysis.

The choice of this decision-making framework has important consequences for the development of the ICLIPS climate and impact models. Firstly, the specification of 'intolerable' impacts of climate change requires that the simulated impacts for a wide range of climate scenarios can be expressed by means of aggregated impact indicators. Non-monetary indicators should be used whenever established market prices do not exist. Secondly, the climate and impact models should be capable of providing regionally explicit results that are relevant to policymakers. Finally, numerical efficiency is a crucial requirement for all model components due to the huge numerical burden associated with the computation of the set-valued solutions (see Bruckner et al., 1999; 2003a).

These partially conflicting goals motivated the development of the ICLIPS climate model (Bruckner et al., 2003b) and of the reduced-form climate impact model that consists of an extensive set of sector-specific CIRFs. A CIRF depicts the response of a climate-sensitive system to changes in selected indicators of the global climate system. It provides the integrated ICLIPS model with information on anticipated climate impacts for a wide range of scenarios. The CIRFs presented here reproduce the aggregated results of multiple

simulations with geographically explicit, process-based impact models in an efficient way. They require neither the prescription of a functional form nor the conversion of non-market impacts into monetary units.

There are three principal application modes for CIRFs. Firstly, they can be used in ‘forward mode’ to determine the likely impacts of a specific climate state or scenario, analogous to standard applications of process-based climate impact models. Secondly, in ‘overview mode’, a CIRF allows the detection of possible non-linear responses of a system to changes in the forcing variables. The joint effect of the driving variables and possible trade-offs can also be easily identified. Finally, and most important within ICLIPS, a CIRF can be used in ‘inverse mode’ to determine the subset of climate states where a previously defined impact guardrail is not violated. The ICLIPS integrated assessment model can determine the bundle of permitted emission paths by applying that subset, denoted as a ‘tolerable (climate) window’, to constrain the respective variables in the ICLIPS climate-economy model. Examples of all application modes of CIRFs will be presented in Section 3. For results of the integrated ICLIPS model, see Toth et al. (2003).

Note that similar terms like CIRFs have been previously used in different contexts (see, e. g., Huntley et al., 1995; Carter et al., 1994). The main new aspects in our approach are the use of non-monetary aggregated indicators for the specification of ‘unacceptable’ impacts of climate change, the application of geographically explicit impact models for the computation of aggregated impacts, the concise representation of simulation results independent from a specific emission scenario, and the inclusion of maximum information from GCMs on the spatial and seasonal variability of climate change. These features allow us to include constraints to climate impacts in inverse analyses of the climate change problem within the TWA framework.

2.2. CIRFS: CALCULATION PROCEDURE AND CLIMATE INPUT

In order to make both the computation and the presentation of a CIRF feasible, the state space needs to be limited to a few dimensions that can be scanned efficiently. It is recognized that the response of many systems to climate change is contingent upon socioeconomic factors. However, by focussing the impact investigations on those sectors, indicators, and regions where changes in climatic indicators are the prime driving force and socioeconomic factors are of less importance, it is deemed sufficient to consider only climatic input variables in the CIRFs presented here. Below, we discuss the climate input to the CIRFs. A list of impact indicators, i. e., the output variables of the CIRFs in the ICLIPS model, will be presented in Section 3.

The development of CIRFs draws on earlier efforts to develop ‘ecological response functions’ for specific climate change scenarios (Toth, 1996; Toth et al., 2000) and agricultural ‘response-surface diagrams’ that link crop yields

to incremental changes in annual temperature and precipitation (van Minnen et al., 2000). In order to base the CIRFs on more consistent climate scenarios, we apply the scaled scenario approach. Pseudo-transient climate change scenarios for arbitrary emission trajectories are constructed by scaling fixed climate change patterns to the time-dependent change in AGMT (Santer et al., 1990; Carter et al., 1994) as determined by a reduced-form climate model such as the ICLIPS climate model. Climate change patterns are derived from coupled atmosphere-ocean general circulation model (AOGCM) experiments. They state the regional change in pertinent climate variables for a unit change in AGMT, thus assuming an approximately linear relationship between global and regional climate change. As actual scaling variable for the climate change patterns, we use the *normalized* change in AGMT, i. e., the *absolute* change in AGMT divided by the so-called equilibrium climate sensitivity of the respective GCM to a doubling of equivalent greenhouse gases concentrations, $\Delta T_{2\times\text{CO}_2}$. Doing so, different climate sensitivities between GCMs are consistently taken into account.

It is often assumed that the scaled scenario approach is a good approximation for temperature but that it works poorly for precipitation. Recent research, however, no longer supports this view. Dai et al. (2001) compare regional patterns of seasonal-mean temperature and precipitation changes from GCM ensemble experiments between a business-as-usual and a greenhouse-gas stabilization scenario. The patterns are highly correlated, with correlation coefficients $r \approx 0.99$ for temperature, and $r \approx 0.93$ for precipitation. The main difference between this study and others that found lower correlations (e. g., Mitchell et al., 2000) is the use of ensemble experiments for both the business-as-usual and the stabilization experiments. The scaled scenario approach is further discussed in Bruckner et al. (2003b) with regard to the ICLIPS climate model; for a more general discussion, see Mitchell et al. (1999), and Smith and Pitts (1997).

The computation of a CIRF involves the application of a geographically explicit impact model to a representative subset of plausible future climate states. Climate change patterns for monthly averaged temperature, precipitation and cloudiness are scaled to the (normalized) change in AGMT and superimposed onto the baseline climate. In this way, both the seasonal and the spatial variability in the climate change signal as simulated by the GCM are consistently taken into account. The baseline climate is represented by the 1961-1990 mean climatology constructed by New et al. (1999) that covers all land areas except Antarctica on a 0.5° latitude by 0.5° longitude grid. In the present version of CIRFs, sub-monthly climate characteristics and interannual climate variability as well as changes in these characteristics are not considered. The main reasons are the lack of respective data for the former, the need to define probabilistic impact indicators for the latter, and the associated demand for computing resources.

AOGCMs are the most reliable sources for projections of future climate under increasing greenhouse gas concentrations. However, they have not been designed to provide direct input for process-based models used in assessing regional impacts of climate change. The main causes of inconsistencies at the interface of climate models and impact models are the use of different spatial and temporal scales, interpolation and extrapolation from a restricted number of climate simulations, and the imperfect simulation of the current climate by AOGCMs (Robock et al., 1993; Henderson-Sellers, 1996; von Storch, 1995). Although various advanced downscaling techniques exist (e. g., limited area models and empirical-statistical approaches), the available computer resources and calibration data still do not allow their application at the global scale. The GCM results are therefore mapped onto the finer grid of the baseline climatology by linear interpolation between GCM grid cell centers.

We construct absolute climate change patterns for temperature by directly using the simulated temperature anomalies between the GCM scenario and the control runs. For precipitation and cloud cover, we apply relative climate change patterns as default. They represent the simulated percentage change as a multiplier to the observed value, thus avoiding negative values and compensating for scaling-independent errors. This procedure may, however, result in serious overestimates of future precipitation if present precipitation is underestimated in the GCM control simulation, and if significant precipitation increases are simulated for the climate change scenario (Carter et al., 1994). For these reasons, we use the ratio of simulated to observed baseline precipitation, λ , as criterion for a smooth shift to using the absolute precipitation difference. The relative change is applied for $\lambda \geq 1$, the absolute change for $\lambda = 0$, and an intermediate value for $0 < \lambda < 1$. Note that the use of absolute vs. relative patterns of precipitation change may have noticeable effects on the results of impact assessments (Alcamo et al., 1998, p. 93).

We account for differences in climate change projections between GCMs by using climate change patterns from different GCM integrations. Due to the limited space available here, we confine the presentation to results from recent integrations of two AOGCMs that are available through the IPCC Data Distribution Centre. One set of climate change patterns is taken from the ECHAM4GGa1 experiment, performed with ECHAM4/OPYC3 at T42 resolution (Bacher et al., 1998; Roeckner et al., 1996), the other one is taken from the average of the HadCM2GGaX ensemble experiment, performed with HadCM2 on a 2.5° latitude by 3.75° longitude grid (Johns et al., 1997). For both GCMs, the simulation results for a scenario that involves a 1% per annum increase in greenhouse gas concentrations from 1990 to 2099 are compared to the unforced control simulations. More details on the construction of the climate projections can be found in Füssel and van Minnen (2001).

All CIRFs in this paper use the normalized change in AGMT as their main input variable. Even though CIRFs are presented at different spatial aggre-

gation levels, the scaled scenario approach allows the use of the normalized change in AGMT as a common input variable. Depending on the respective impact sector, the data requirements of the impact model, and the information available from other components of the integrated model, additional input variables may be included. The CIRFs for natural vegetation and for crop production use the atmospheric CO₂ concentration as a second input factor because it affects the behavior of crops and natural ecosystems (Jones et al., 1998). Although increasing CO₂ is the principal cause of global climate change, the relationship between CO₂ concentration and the transient change in AGMT is not one-to-one, even for a fixed climate sensitivity, due to the influence of non-CO₂ greenhouse gases and aerosols, and the thermal lag of the climate system. The CIRFs for water availability do not consider the CO₂ concentration.

The scaled scenario approach requires that a CIRF is linked to a specific GCM experiment. However, CIRFs allow the assessment of potential impacts of arbitrary emissions scenarios by applying an efficient climate model to compute the associated changes in AGMT and CO₂. The domain of the CIRFs presented here is chosen so that it includes the trajectories of all emission scenarios of the Special Report on Emissions Scenarios (SRES) (IPCC, 2000) up to the year 2100. AGMT varies in 21 steps from the baseline value up to a $1.6 \cdot \Delta T_{2 \times \text{CO}_2}$ warmer climate. This range corresponds to 4.5 °C for both GCMs considered here. The CO₂ concentration varies in 23 steps from 325 ppm (the average concentration of the year 1970 used as the reference value) up to 1200 ppm.

2.3. IMPACT MODELS

In this section, we present an overview of the impact models used to compute the CIRFs. We focus on those aspects which are relevant in the ICLIPS framework and refer the reader to other sources for details.

Climate impacts on natural vegetation, crop production, and freshwater availability are assessed by applying adapted versions of BIOME 1, the FAO crop suitability model, and WaterGAP 1.1, respectively. A common characteristic of these models is that they use soil information and daily climate data as inputs. Quasi-daily climate time series are derived from monthly averages by linear interpolation (for temperature), and by spline interpolation (for precipitation and cloudiness). The results of BIOME 1 and the FAO crop model are also affected by atmospheric CO₂. All models include a hydrological sub-model, although its implementation differs somewhat between the models. The models are globally applicable, a spatial resolution of 0.5° latitude by 0.5° longitude being used for the computations, and they are computationally efficient.

Natural vegetation

The BIOME 1 model (Prentice et al., 1992), as modified for the IMAGE 2 model (Alcamo et al., 1998), is used to simulate the potential vegetation distribution for current and future climate states. BIOME 1 is a biogeographical vegetation model, developed from physiological considerations. The model simulates the large-scale distribution of biomes, assuming an equilibrium between vegetation and environment.

BIOME 1 proceeds in two steps. In the first step, the model uses a set of climate indices and related constraints to determine which plant functional types (PFTs) can exist in a grid cell. These indices (e. g., temperature characteristics during the growing season) function as an environmental sieve, based on the non-violation of any of the constraints. PFTs are classes of plant species, grouped by morphological (e. g., broad-leaved vs. coniferous) and phenological characteristics (e. g., evergreen vs. summergreen). In the second step, the 16 PFTs are grouped into 14 biomes (for a complete list, see Figure 4). A dominance hierarchy is included for this purpose as a proxy for plant competition between PFTs. The original BIOME 1 model has been modified to include a CO₂ dependency of the moisture thresholds (Alcamo et al., 1998). Enhanced levels of CO₂ increase the water use efficiency of plants that allows them to grow under more arid conditions.

Progress has been made recently in developing dynamic vegetation models (e. g., Foley et al., 1996). Such models include a higher level of physiological detail that enables them to simulate transient vegetation changes and the carbon dynamics of ecosystems. Kirilenko and Solomon (1998) compare the vegetation response to long-term climate change as simulated by BIOME 1 and by MOVE, a global biome model that explicitly includes vegetation migration and succession. They find that the biome changes simulated by the two models are quite similar, with the overall Kappa statistic (a coefficient for pairwise agreement between two classification ratings) lying between 0.94 and 0.99.

The cited results imply that dynamic aspects are of minor importance for the impact indicators defined for the ICLIPS model because they are solely based on the long-term distribution of biomes (cf. Table II). We thus regard the application of BIOME 1 as justified here. Equilibrium vegetation models have, however, only limited value for determining the timing of vegetation changes. Consequently, statements on the unsuitability of a future climate for the current biome below do not aim to pretend that the actual vegetation change will occur exactly at the specified date. The transition from one biome to another may well take several decades, and it will probably not be a smooth and uniform process. Since the vast majority of emission scenarios lead to continued increases in AGMT and CO₂ levels far into the 22nd century, we nevertheless must expect that the changes simulated for a transient climate state in the 21st century will eventually be realized.

Agricultural crop production

The FAO crop suitability model, as adapted for IMAGE 2 (Alcamo et al., 1998), is applied to assess the risks of climate change for agricultural production and food security.

The model proceeds in two steps. In the first step, which is similar to BIOME 1, the model computes the potential distribution of the 19 most important crops worldwide under rain-fed conditions. By applying crop-specific constraints to a set of agro-climatic indices for temperature and moisture availability defined in FAO (1981), it determines those grid cells where the environmental conditions are adequate for growing specific crops. In the second step, the model computes the potential rain-fed production for all suitable crops, based on the growth functions of de Wit (1978).

The original detailed formulation has been adapted to enable the computation of crop growth at the global scale. The production is determined by the net biomass production, defined as gross photosynthesis minus plant respiration (van Minnen et al., 2000). Photosynthesis is governed by temperature, moisture availability, soil conditions, and the CO₂ concentration in the atmosphere. Soil reduction factors that are taken into consideration are fertility, salinity, acidity, rooting depth, and drainage conditions according to the FAO (1988). Plant respiration depends on total biomass and temperature (Leemans and van den Born, 1994). Atmospheric CO₂ affects the distribution and production of crops in two ways. Firstly, increased levels of CO₂ reduce transpiration rates and thus increase the water use efficiency of plants (Alcamo et al., 1998). Secondly, the so-called CO₂ fertilization effect describes the direct stimulation of photosynthesis under enhanced CO₂ levels (for details, see Klein Goldewijk et al., 1994).

The FAO crop suitability model computes the rain-fed yield of the most important annual crops. Multicropping and irrigated agriculture are not included in the present model version. Consideration of adaptation to changing climate conditions is rather limited. Since the model assumes an optimal planting date by design, seasonal adjustments in response to climate changes are taken into account. In addition, some of the aggregated indicators apply simple decision rules to allow for switching to more suitable crops (see Table III). More detailed adaptation assessments of the agricultural sector would require a rather different class of models that include the effects of demographic, socio-economic, and technological developments on the demand and supply of food, as well as the interdependencies among different regions.

Freshwater availability

The global hydrological model WaterGAP 1.1 (Döll et al., 1999) has been used to simulate global and regional water availability. Water availability is computed at the level of river basins as the total runoff (i. e., surface runoff and groundwater recharge) of all grid cells therein.

Routing between grid cells is not included in this model version. The daily water balance of each grid cell is therefore computed as

$$\frac{\partial S}{\partial t} = P_{eff} - E_a - R,$$

where S is the actual water content in the effective rooting zone, P_{eff} the effective precipitation (rainfall plus meltwater), E_a the actual evapotranspiration, and R the surface runoff. Both E_a and R are functions of S , which itself is calculated from these variables, based on the previous time step. E_a is calculated from the potential evapotranspiration, E_p , and the total available soil water content, S_{max} , as

$$E_a = \min \left(E_p, E_{p,max} \cdot \frac{S}{S_{max}} \right),$$

whereby $E_{p,max} = 10$ mm/d, and S_{max} is the product of the vegetation-specific rooting depth and the available water capacity in the uppermost metre of the soil (Batjes, 1996). Runoff R is calculated according to Bergström (1995) as

$$R = P_{eff} \cdot \left(\frac{S}{S_{max}} \right)^\gamma,$$

with P_{eff} as defined above.

WaterGAP is a reduced-form model with only one calibration parameter, the runoff coefficient γ , that was adjusted to time series of annual discharges of 41 large watersheds (Grabs et al., 1996). A regionalization algorithm is then used to assign values to the other river basins.

Note that the present version of WaterGAP does not consider the CO_2 concentration. Increasing CO_2 levels reduce the evapotranspiration rates of plants and thus partly compensate the additional water loss due to increasing temperatures. This effect is particularly relevant in dry areas. The simulated decreases in runoff may therefore be slightly overestimated. Nevertheless, precipitation will be the dominant factor in determining the water availability in all watersheds around the world.

3. Results

In this section, we present simulated climate impacts on natural vegetation, agricultural production potentials, and freshwater availability. Due to the large number of impact indicators, countries, and sources of climate scenarios that are considered in the ICLIPS model, only selected findings can be shown. For each impact sector, CIRFs for one important impact indicator are presented as

TABLE I

Climate change in selected countries and regions. Data refer to the simulated changes in annual mean surface temperature (ΔT), precipitation (ΔP), and cloud cover (ΔC) in response to a doubling of the equivalent CO_2 concentration. The associated change in AGMT, denoted as the equilibrium climate sensitivity, $\Delta T_{2\times\text{CO}_2}$, is $+2.8$ °C for both GCMs.

	Land surface*	Brazil	China	Germany	India	Russia	SACU**	USA
<i>ECHAM4</i>								
ΔT [°C]	+4.4	+4.1	+4.7	+4.2	+3.4	+6.4	+4.0	+4.4
ΔP [%]	+6.9	-3.9	+12.0	-0.8	+27.2	+16.9	-6.5	+3.5
ΔC [%]	+1.2	-0.5	+0.1	-2.7	+7.9	+2.1	+1.1	-0.9
<i>HadCM2</i>								
ΔT [°C]	+3.9	+4.1	+3.6	+2.9	+4.5	+4.3	+4.5	+3.5
ΔP [%]	+3.4	-0.4	+13.1	-1.8	-16.3	+12.3	-6.2	+16.5
ΔC [%]	-0.7	-5.4	± 0.0	-1.4	-5.0	+1.4	+8.6	+5.8

*All countries except Antarctica and Greenland.

**South African Customs Union; comprises the Republic of South Africa, Namibia, Botswana, Lesotho, and Swaziland.

the main result. We focus our assessment on a limited number of countries that cover a broad range of climate regimes and socioeconomic conditions (see Table I). The climate scenarios are based on transient experiments with the AOGCMs ECHAM4 and HadCM2. An interactive computer tool has been developed to present simulation results for all indicators and countries and for a wider range of climate scenarios. It is available on CD-ROM from the first author of this paper.

3.1. IMPACTS ON NATURAL VEGETATION

The BIOME 1 model as adapted for IMAGE 2 is applied to determine the CIRFs for natural vegetation, i. e., to compute changes in the global distribution of biomes for a given climate and CO_2 concentration. Through aggregation and spatial masking of the original model results, we define various impact indicators listed in Table II. Each of them emphasizes different aspects of the simulated vegetation impacts.

We focus here on the indicator ‘protected area with biome change’ but we also summarize the response of individual biomes. The chosen indicator, which may alternatively be termed ‘percentage of endangered nature reserves’, considers only protected areas contained in the most recent version of the respective UN list (IUCN, 1998). We regard this indicator as particularly policy-

TABLE II

Indicators of climate change impacts on natural vegetation. All impacts are expressed as percentage of the baseline area.

Indicator	Definition
Stable biome area	Percentage of an individual biome's present extent that remains climatically suitable. Newly suitable areas are not taken into account.
Total biome area	Total potential area of an individual biome. Losses within the present range can be (over-) compensated by newly suitable areas elsewhere. Migration obstacles etc. are not considered.
Stable forest area	Percentage of the present forest area that remains suitable for forest growth (whereby a change from one forest biome to another one is permitted).
Total forest area	Total potential forest area. Losses within the present range of forests can be (over-) compensated by newly suitable areas elsewhere.
Land area with biome change	Percentage of the land surface where the present biome is no longer viable under altered climate conditions.
Non-agric. area with biome change	As before except that areas used for agriculture are not considered.
Protected area with biome change	As before except that only protected areas are considered.

relevant for various reasons. Firstly, the legal protection of an area is a clear statement on the societal appreciation of its present ecological features. A fundamental vegetation change is thus likely to be valued negatively. Secondly, non-climatic human-induced stresses, for instance land reclamation, are generally less important in protected areas than elsewhere. Similar indicators have been used in previous climate impact assessments on vegetation (Leemans and Hootsmans, 1998; Martin, 1996; Villers-Ruíz and Trejo-Vázquez, 1998).

Figure 1 shows the globally averaged response of the indicator 'percentage of endangered nature reserves' to changes in AGMT and CO₂ concentration. The *response surface diagram* on the left depicts the dose-effect relationship between the two forcing variables of the CIRF on the horizontal axes and the impact indicator on the vertical axis by interpolating across the points at the intersection of the selected increments. Using a geographical analogue, a response surface diagram represents a 3-dimensional landscape model that shows the 'height' of an impact for every possible 'location' in the (2-dimensional) climate space. The bottom left-hand corner of the response surface diagram in Figure 1 corresponds to the baseline climate. The relation-

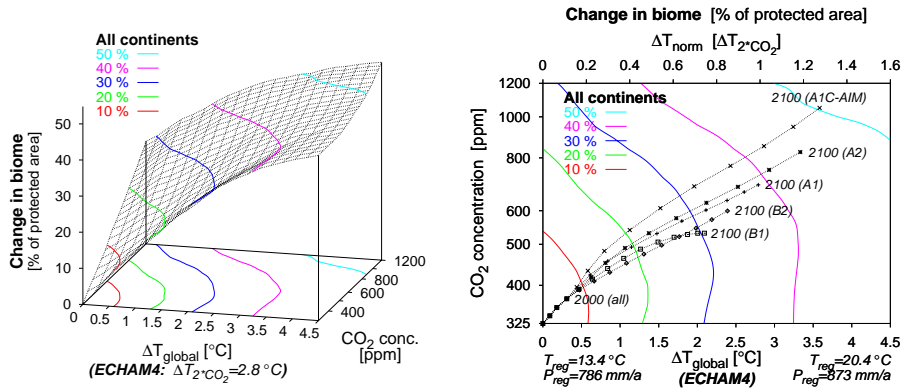


Figure 1. Globally averaged response of natural vegetation in protected areas to a wide range of future climate states. *Left*: Response surface diagram. *Right*: Impact isoline diagram with time trajectories for various SRES emissions scenarios. (A detailed explanation of all diagrams is given in the text.)

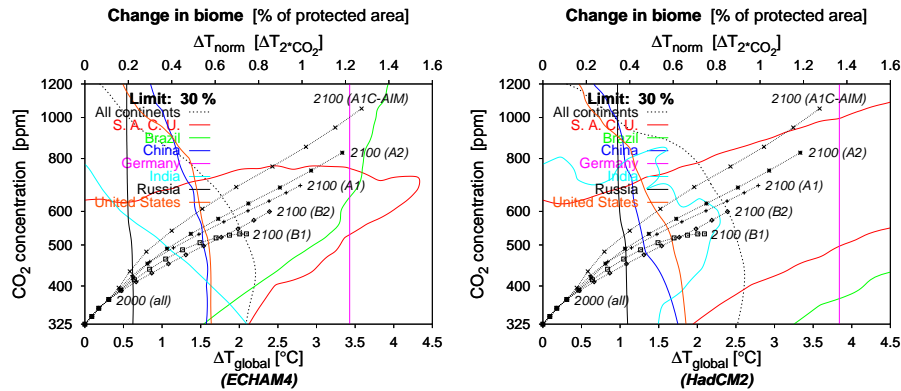


Figure 2. Impact isoline diagrams, depicting the climate windows associated with an illustrative impact constraint that limits vegetation changes to 30% of protected areas in each region, based on climate scenarios from ECHAM4 (*left*) and HadCM2 (*right*).

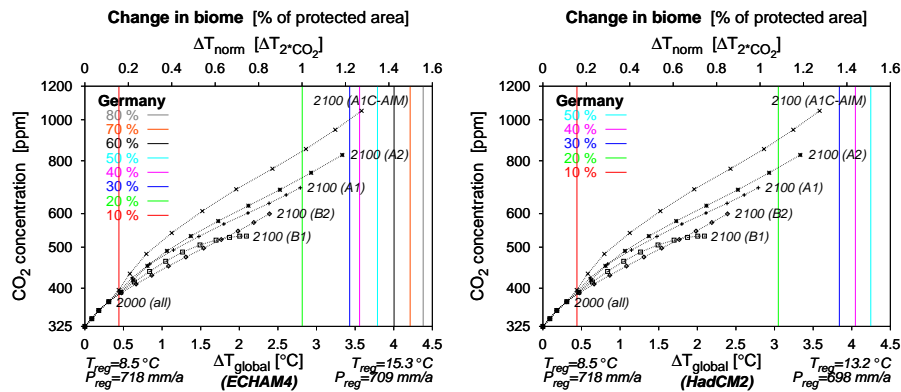


Figure 3. Impact isoline diagrams for vegetation change in Germany, based on climate scenarios from ECHAM4 (*left*) and HadCM2 (*right*).

ship between each forcing variable and the global impact indicator is smooth and monotonically increasing. The combined effect of changes in both forcing variables is generally larger than the effect of each individual input variable but less than their sum. The colored isolines connect points on the response surface for which the same aggregated impacts are simulated. In this example, they represent the loss of the current biome in 10 %, . . . , 50 % of protected areas worldwide. Response surface diagrams provide an easily understandable visualization of a CIRF. Their 3-dimensional nature, however, is less suited for inverse applications and for sensitivity analyses.

The *impact isoline diagram* (right-hand plate of Figure 1) shows the projection of the isolines from the response surface diagram onto the domain of the CIRF. In the geographical analogue, an impact isoline diagram corresponds to a topographical map with contour lines. Some additional information is given in the impact isoline diagrams presented here. Firstly, below the diagram we state the annual mean temperature and precipitation in the considered region both for the baseline climate and for the endpoint of the climate domain. This reminds the reader that the scaled scenario approach considers changes in all pertinent climate variables simultaneously. Secondly, we show the climate evolution of the four marker scenarios (A1, A2, B1, and B2) and an additional high-emission scenario (A1C-AIM) specified by the SRES team (IPCC, 2000), as computed by the ICLIPS climate model. The time trajectories start at the bottom left corner of the diagram that represents the reference climate and CO₂ concentration. Dots mark their evolution until 2100 in 10-year steps. Whenever a scenario trajectory intersects an impact isoline, it implies that the corresponding guardrail is crossed. The ‘50 % guardrail’ (denoted by the light blue isoline in the top right-hand corner) is, for instance, violated under the A1C-AIM scenario around the year 2100.

Whereas response surface diagrams and impact isoline diagrams are based on the same information, the latter type is better suited for inverse analyses of climate change. The boundary of the climate window associated with a specific impact guardrail is constituted by the respective impact isoline that separates the domain of the CIRF into two regions: one where the simulated impacts lie below the guardrail, and another one where they lie above.

Figure 2 presents the regional sensitivities of natural vegetation. The impact isoline diagrams refer to an illustrative ‘30 % guardrail’ in each country, based on the results of both GCMs. We now take a closer look at the country-specific isolines for ECHAM4 in the left-hand diagram. Here, the isoline denoted ‘All continents’ (which is identical to the ‘30 %’ isoline in Figure 1) can be used as a reference for the regional sensitivities. In Germany and Russia, vegetation change is almost exclusively driven by changes in climate (primarily temperature). To a somewhat lesser extent, this is also the case in the USA and China. Vegetation in India is affected by changes in both climate and CO₂ concentration. The response in the South African Customs Union (SACU) may be

surprising at first sight. Whereas the vegetation is highly sensitive to changes in either climate or CO₂ alone, the effect of combined changes is much lower for most scenarios. This response pattern points to a compensation between the effects of climate changes that decrease the water availability in the region, and those of rising CO₂ levels that increase the water use efficiency of plants. A similar pattern is simulated for Brazil.

Due to the varying regional sensitivities, the point in time when the illustrative guardrail is violated under the SRES scenarios differs vastly across countries. Around the year 2020, the climate is already expected to be no longer suitable for the 'current' vegetation (i. e., in equilibrium with the baseline climate) in 30 % of the protected area of Russia. In contrast, this guardrail is not violated in Brazil by any of the scenarios until 2100. The right-hand diagram of Figure 2 presents the country-specific isolines based on the results of HadCM2. Whereas the isolines for ECHAM4 and HadCM2 are similar at the global level and for some regions, significant differences are simulated for other regions.

Figure 3 shows that the vegetation in Germany exhibits a threshold behavior for both GCM projections. Up to a certain amount of climate change (about 3 °C increase in AGMT), the model projects only limited changes (less than 20%) in the distribution of biomes. Beyond that threshold, widespread vegetation changes must be expected. Such a behavior cannot be identified by traditional climate impact assessments based on point estimates.

Figure 4 presents additional information on the response of specific biomes for selected regions. The *area balance diagrams* show the potential area of each biome in a future climate state (after equilibration) compared to the baseline climate. The circles depict the baseline area of each biome whereas the lower and upper bars show the 'stable area' and the 'total area' in the future, respectively (see Table II). The underlying climate changes are stated above the diagrams. For the year 2100 of the SRES A1 marker scenario chosen here, the ICLIPS climate model simulates a CO₂ concentration of 690 ppm and a (transient) increase in AGMT that equals the climate sensitivity of the respective GCM.

We discuss the global area balance diagram (top left-hand diagram in Figure 4) only. Due to their varying climatic requirements, biomes show very different responses. Tropical evergreen forest, for instance, is not expected to lose a large fraction of its current extent, and tropical woodland may even expand considerably into areas that are currently unsuitable. The prospects are worse for some high-latitude biomes. No part of the present range of wooded tundra and cool coniferous forest is modeled as remaining suitable for these biomes in the long term. The *total* potential area of wooded tundra (and of tundra) is also drastically reduced. Obviously, the realization of such a scenario would dramatically alter the surface of the Earth.

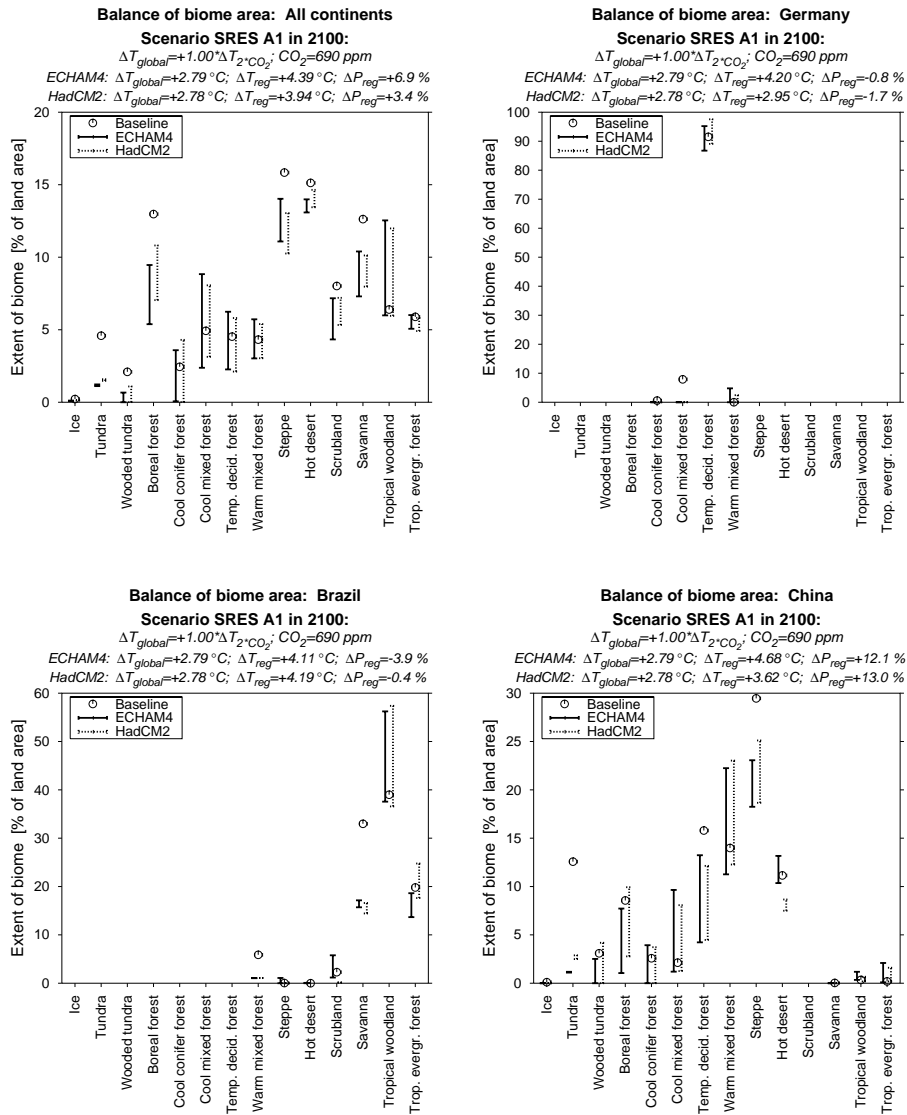


Figure 4. Area balance diagrams, depicting the potential extent of all biomes for the baseline climate (1961-1990), and for the climate simulated by ECHAM4 and HadCM2 in the year 2100 under the SRES A1 marker scenario. The lower end of the bar refers to the stable area of a biome whereas the upper end refers to the total area, including newly suitable regions. ΔT_{global} , ΔT_{reg} and ΔP_{reg} denote the change in global mean temperature, regional mean temperature and regional precipitation, respectively. $\Delta T_{2 \times CO_2}$ is the GCM-specific climate sensitivity (for a doubling of the equivalent CO_2 concentration). *Top left*: All continents. *Top right*: Germany. *Bottom left*: Brazil. *Bottom right*: China. (Note the different scaling of the y axis.)

TABLE III

Indicators of climate change impacts on crop production (b: basic indicator for a specific crop; a: indicator aggregated across crops).

Indicator	Definition
Crop yield (b)	Harvestable part of dry weight production under local climate and soil conditions [t/ha]
Suitable area (b)	Area where a crop can grow, assuming 10 % of its maximum yield as the minimum threshold [% of total area]
Maximum food energy (a)	Maximum caloric yield, using the caloric yield as the criterion for crop allocation in each grid cell [Gcal/ha]
Maximum crop performance (a)	Performance of the 'best' crop, using the actual performance of a crop (expressed as a percentage of its maximum yield) as the criterion for crop allocation [% of max. yield]
Weighted crop performance (a)	Performance of all crops (within the present cultivated area), whereby the result for each crop is weighted with its present share in the agricultural output of a country [% of max. yield]

3.2. IMPACTS ON AGRICULTURAL PRODUCTION

The FAO crop suitability model as adapted for IMAGE 2 is applied in the ICLIPS framework to determine the suitable area and the potential rain-fed production of the 19 most important crops worldwide. We define various indicators to express the sensitivity of agricultural production to climate change (see Table III). The crop-specific ('basic') indicators present an indispensable source of detailed information whereas the aggregated indicators express the overall impacts on the agricultural sector under different assumptions with respect to crop switching. All indicators, except the last one ('weighted crop performance'), are computed both for the total land area of a region (e. g., a country) and for the current cultivated area (based on Ramankutty and Foley, 1998). We consider the latter case to be particularly relevant because significant shifting of the areas used for agriculture will often be difficult due to, for instance, the unavailability of the required infrastructure or conflicts with other land uses.

Here we focus on the indicator 'weighted crop performance' that describes the response of the currently important crops in the cultivated area of a country. As crop switching is not allowed for this aggregated indicator, it describes the sensitivity of the present agricultural sector to altered climate conditions under rather pessimistic assumptions concerning adaptation. Both the CIRFs and the impact diagrams used to present them are defined in the same way as for natural vegetation.

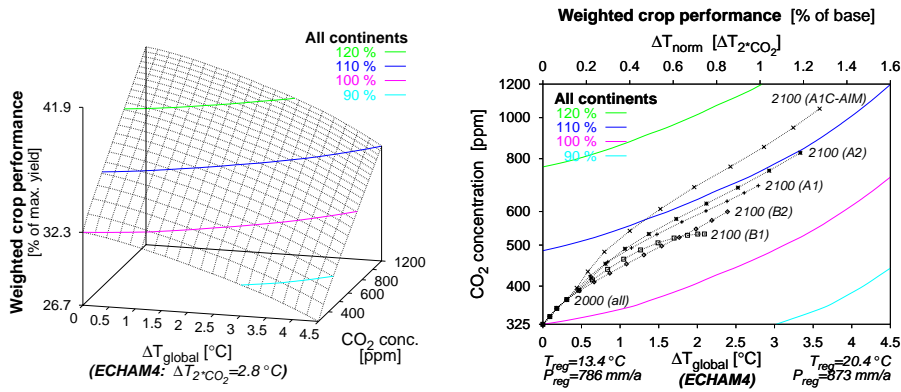


Figure 5. Impacts of climate change on global crop production for a wide range of future climate states. *Left*: Response surface diagram; *Right*: Impact isoline diagram with time trajectories for various SRES emissions scenarios. (A detailed explanation of all diagrams is given in the text.)

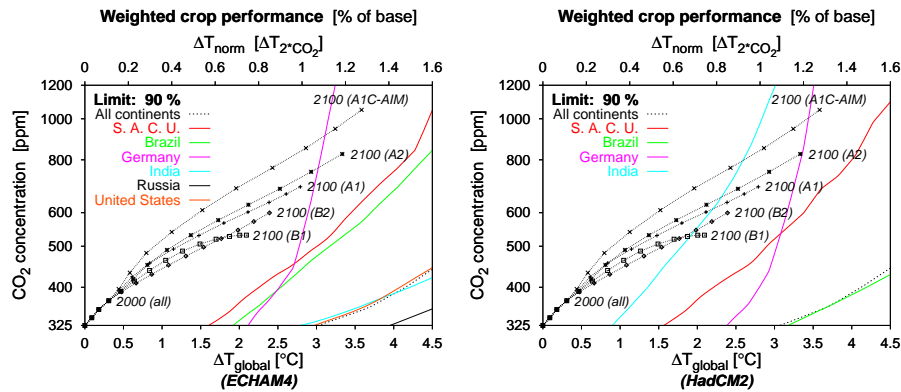


Figure 6. Impact isoline diagrams, depicting the climate windows associated with an illustrative impact constraint that limits weighted losses of current crops to 10% in each region, based on climate scenarios from ECHAM4 (*left*) and HadCM2 (*right*).

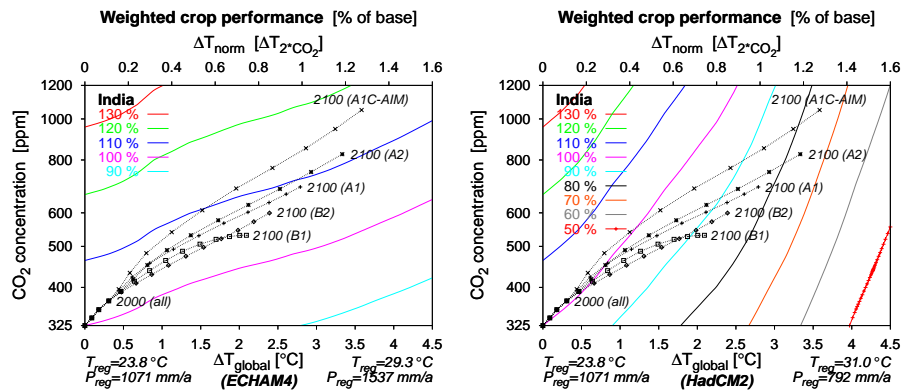


Figure 7. Impact isoline diagrams for crop production in India, based on climate scenarios from ECHAM4 (*left*) and HadCM2 (*right*).

Figure 5 provides an overview of the results by showing the globally averaged response of the chosen indicator. The changes in temperature, precipitation, and cloudiness simulated by the ECHAM4 model lead to slightly decreasing production levels of the currently important crops. If changes in the CO₂ concentration are also considered, production gains of 5 to 15% compared to the baseline are simulated for the year 2100 under all scenarios, i. e., the beneficial effects of enhanced CO₂ levels compensate the climate-induced losses. The climate windows associated with any reasonable impact guardrail at the global level are so large that they would not effectively constrain the computation of emissions corridors in a TWA application.

Figure 6 shows the impact isolines of all countries considered here for an illustrative guardrail of 90 % of the baseline value, i. e., a 10 % loss of the production potential. The left-hand diagram refers to the ECHAM4 climate projection, and the right-hand plate is based on the results of HadCM2. According to the model results, Germany and India are the only countries considered that must expect significant reductions to their agricultural potential. The results for Germany differ only slightly between the climate scenarios, and the impact constraint is violated in at least one of the SRES scenarios for both climate projections. Crop-specific results (not presented here) show that it will become difficult to grow certain presently important crops (e.g., winter wheat) because the projected temperature increase leads to a disappearance of the required chilling period.

Crop responses between the two climate projections differ most significantly for India (see Figure 7). Based on the ECHAM4 results, the illustrative guardrail is not crossed in any of the SRES scenarios whereas for the HadCM2 results, it is violated in all of them. This difference can be explained by the large discrepancies in the simulated precipitation changes between the two GCMs.

Figure 8 (top left-hand diagram) supplements the results conveyed by the aggregated indicators. It shows the global balance of the suitable area for each crop within the current cultivated area based on simulations of both GCMs for the year 2100 of the SRES A1 marker scenario. Whereas the area suitable for tropical crops (e. g., tropical maize, cassava) increases at the global scale, a significant fraction of the current area for temperate crops (e.g., wheat, temperate maize) is projected to become unsuitable.

We now take a closer look at the crop-specific results for India depicted in Figure 8 (top right-hand diagram). The area suitable for the rain-fed production of rice, the most important staple crop, remains largely unaffected based on the ECHAM4 projection, yet it decreases by almost 50% based on the HadCM2 projection for the year 2100 under the SRES A1 scenario. It is very likely that irrigated rice production, accounting for about 45% of the cultivated area, would suffer as well, given the large decreases in water availability associated with this climate scenario. For wheat, the second most important staple crop,

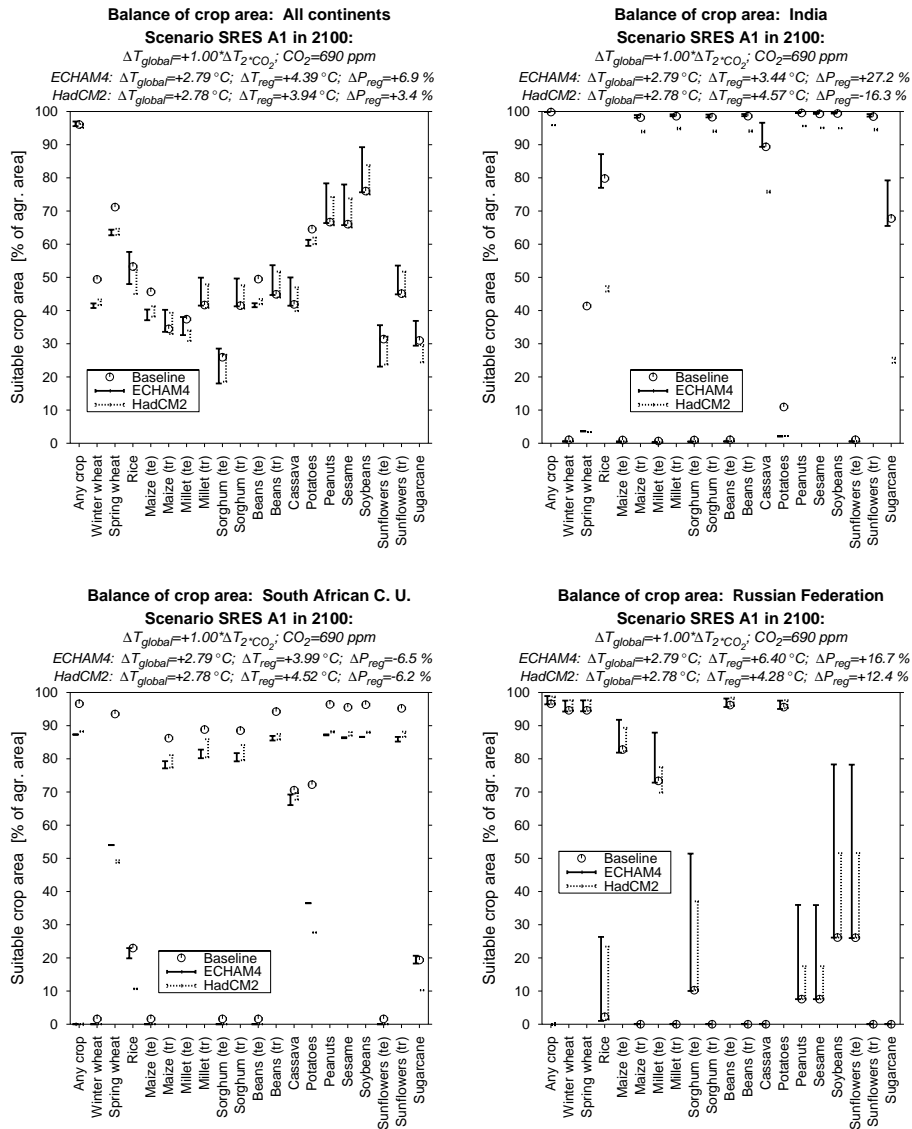


Figure 8. Area balance diagrams, depicting the suitable area of all crops considered (te: temperate, tr: tropical) for the baseline climate and for the climate state simulated by ECHAM4 and HadCM2 for the year 2100 of the SRES A1 marker scenario. *Top left:* All continents. *Top right:* India. *Bottom left:* South African Customs Union. *Bottom right:* Russia. (For an explanation of the diagram, see Figure 4. The suitable area for ‘Any crop’ may be less than 100% of the cultivated area because the former refers to rainfed conditions whereas the latter includes irrigated areas.)

we get a different picture. The simulations project the suitable area to almost vanish by the year 2100 for both GCM projections. These results are basically unchallenged by the fact that about 80% of the cultivated area is irrigated because high temperature rather than water scarcity is the limiting factor here. Even though other tropical crops remain suitable, the realization of such a scenario must be expected to have severe repercussions on society.

Figure 8 (bottom left-hand diagram) shows decreases in the suitable area for all crops in the South African Customs Union. The prospects for Russia's agriculture are rather positive. Figure 8 (bottom right-hand diagram) indicates a significant potential to diversify agricultural production as the current cultivated area becomes suitable for a wider range of crops. Additional simulation results not presented here exhibit that large areas may become newly suitable for agriculture, and yields are expected to increase.

To summarize the findings for agriculture, strong positive and negative responses of currently important crops have been simulated for different regions. The responses are robust across the two GCMs for the global average as well as for many countries. Dramatic decreases in the production of staple crops are simulated for India, yet with major differences between the GCM scenarios. While Germany must expect severe constraints to the production of currently important crops, there is considerable potential for crop switching. Russia will very likely be a 'winner' of climate change as far as agriculture is concerned. For the other countries, slight increases in the agricultural potential are simulated for the SRES scenarios, mainly due to the positive effects of enhanced CO₂ levels.

3.3. IMPACTS ON FRESHWATER AVAILABILITY

The WaterGAP 1.1 model is applied to assess the effects of changing climate on freshwater availability. In general, a decrease in freshwater availability is considered a negative impact. Because increased water availability may result in higher flood frequencies, the opposite effect is not necessarily desirable. An evaluation of flooding risks does, however, require the application of models with a much higher temporal resolution.

WaterGAP calculations are based on water basins. As water cannot be easily transferred over basin boundaries, this is the spatial unit which is most appropriate for water-related analyses. In order to state results at the country level, a representative basin has been identified for each country. For most countries, this basin covers a significant part of the area and the population.

Table IV presents aggregated simulation results. For each country, the table states the representative river basin, annual values for important climatic variables averaged over the basin area, and the annual freshwater availability. The GCM-based results refer to the climate state when AGMT is increased by $1.6 \cdot \Delta T_{2 \times CO_2}$, relative to the baseline climate. This corresponds to the

TABLE IV

Simulated annual mean freshwater availability in the current climate and in a future climate state characterized by a global mean temperature increase of $1.6 \cdot \Delta T_{2 \times \text{CO}_2}$, based on two GCMs (see text). T : temperature; P : precipitation; W : water availability; ΔX : change in X relative to the current climate.

Country	Brazil	China	Germany	India	Russia	SACU*	USA
Basin	Amazon	Yangtze	Rhine	Ganges	Volga	Oranje	Mississippi
Current climate							
T [°C]	24.7	11.7	8.2	21.4	3.7	17.8	10.4
P [mm/a]	2096	1030	936	1088	576	359	777
W [mm/a]	1047	538	563	360	175	4.9	140
ECHAM4							
ΔT [°C]	+7.0	+6.2	+7.4	+5.9	+8.4	+6.3	+7.4
ΔP [%]	+10.2	+18.0	-5.9	+52.8	+11.0	-13.0	+7.1
ΔW [%]	+18.4	+22.9	-12.6	+107.2	+37.7	+41.9	± 0
W [mm/a]	1240	661	492	746	241	7.0	140
HadCM2							
ΔT [°C]	+7.3	+5.5	+5.1	+7.9	+5.3	+7.1	+5.3
ΔP [%]	+1.4	+21.6	-3.9	-47.1	+24.9	+1.3	+26.2
ΔW [%]	+0.4	+31.6	-8.7	-83.9	+53.1	-7.1	+72.1
W [mm/a]	1051	708	514	58	268	4.6	241

*South African Customs Union

maximum climate change considered in the CIRFs presented above. The relationship between the (normalized) change in AGMT, the only input variable to the CIRFs for water availability, and the impact indicator is almost linear. For this reason, we do not present impact diagrams for this sector.

Precipitation change is the most important factor for changes in water availability. In dry regions, a significant percentage of precipitation is evapotranspired. This percentage is lower under wet conditions where the dependence of evapotranspiration on precipitation levels off. Consequently, with water availability being defined as that part of precipitation which is not evapotranspired, a percentage change in precipitation typically leads to an even stronger change in water availability. This effect is obvious in most countries considered here.

Increasing temperatures lead to higher evapotranspiration rates and, consequently, to a decrease in water availability. This effect is typically second in importance to precipitation changes. It is clearly visible in scenarios with minor changes in precipitation, e. g., the ECHAM4 scenario for the Mississippi basin in the USA. The only region which does not fit into this picture is the South African Customs Union. For the ECHAM4 climate scenario, WaterGAP simulates a slight increase (in absolute terms) in annual runoff despite decreasing precipitation and increasing temperature. This result can only be explained by considering seasonal climate changes. Since the region has a very low water availability, it is highly sensitive to changes in the seasonality of precipitation.

WaterGAP simulates an increased water availability in most countries investigated here. The only exception is India where large decreases in water availability might be expected. The results for India are, however, highly sensitive to the choice of the climate scenario. Whereas ECHAM4 simulates a precipitation increase of 53% in the Ganges basin, HadCM2 projects a decrease of 47% for the same change in AGMT. The corresponding changes in freshwater availability are even more severe. Since the Ganges basin is densely populated and has large irrigated areas, a strong decrease in water availability (such as projected for the HadCM2 scenario) must be regarded as a serious threat to the people in that region.

4. Summary and conclusions

A large variety of approaches has been used over the last decade to estimate impacts of climate change. Each of those approaches has its own merits and shortcomings and improves our understanding of the complex relationships between climate (change and variability), the biophysical environment, and human societies. There is an increasing number of scientifically rigorous impact studies in some regions (Western Europe, United States) and in certain sectors (agriculture, sea-level rise), but the global picture of climate change risks remains patchy. The concept of CIRFs and the results presented in this paper are intended to provide additional tools that are directly applicable in the inverse modeling framework and potentially useful in other applications as well.

In contrast to point estimates or functional relationships interpolated from a few points, the CIRFs discussed in this paper specify the responses of climate-sensitive sectors across a wide span of plausible patterns of climate change and, where relevant, CO₂ concentrations. As a result, they can be used directly by social actors to assess the risks of climate change as well as the magnitude and possibility of the adaptation efforts required (where adaptation is possible) to counteract at least part of those impacts. In addition, these CIRFs can also serve

as input to other impact assessment tools for further processing, for example, to derive better, biophysically grounded monetized impact functions.

The CIRFs presented in this paper reveal a wide range of potentially positive and negative effects of climate change across regions, impact sectors, and climate scenarios. Regional and global CIRFs for natural vegetation indicate that ecosystems throughout the world are highly sensitive to the projected changes in climate and atmospheric CO₂. Natural vegetation is found to be most sensitive in high-latitude regions where low (winter) temperatures are the prime limiting factor to vegetation growth. For example, the climate is projected to become unsuitable by 2020 for the current vegetation in 30 % of the protected areas in Russia under all SRES emissions scenarios, while none of these scenarios would produce a similar degree of change in ecosystems in Brazil until 2100. At the global scale, wooded tundra and cool conifer forests are simulated to disappear from (almost) all of their present locations under business-as-usual emissions scenarios. Other biomes, e. g., tropical woodlands, have the potential for considerable expansion into currently unsuitable regions.

The CIRFs for agricultural crop production show that the projected climate changes generally have an adverse impact on the weighted average of the currently important crops. However, for most countries and climate scenarios considered, these climate-induced losses are compensated by the beneficial effects of enhanced CO₂ levels. The response of the currently important crops does not show a clear regional pattern. The vulnerability of the agricultural sector to climate changes is, however, generally higher in (sub-) tropical countries due to fewer alternatives for crop switching and the frequent scarcity of resources to implement effective adaptation measures.

In most cases, a smooth relationship is simulated between the forcing variables and the impact indicator at the given level of aggregation. Some regions and indicators, however, exhibit a threshold behavior. In Germany, for instance, relatively minor impacts on natural vegetation and on the performance of currently important crops are simulated up to a 3 °C increase in AGMT, whereas widespread changes occur beyond that threshold. The identification of a threshold behavior in important impact categories is an important scientific input for climate policy decisions.

In general, impacts agree well for the climate change patterns provided by the two GCMs considered. One notable exception is India where large differences in the precipitation projections between the ECHAM4 and HadCM2 models lead to severe effects for selected staple crops and for the aggregated agroecological potential under the latter pattern but not under the former one.

The above examples show that the CIRFs elaborated in this paper cannot resolve the still vast uncertainties that characterize climate impact assessments. Nevertheless, the CIRF approach provides a framework for considering the bulk of the information available from GCMs for use with impact models to derive regional assessments. The suitability of CIRFs for inverse analyses is

due to their independence from specific emissions scenarios, their reliance on physically consistent climate scenarios, and their biophysical foundation. The concise presentation of extensive model results also facilitates comparisons of different sources of uncertainty, such as those associated with the GCMs, the impact models, etc. In the analysis presented here, however, only one impact model is applied in each sector.

One of the major remaining tasks is to combine these biophysical CIRFs with models of socioeconomic vulnerability and adaptation. Such truly integrated CIRFs are expected to provide policymakers with better insights into the risks of climate change and help them craft effective mitigation strategies.

Acknowledgments

The 1961-90 global mean climatology and the climate change fields from the ECHAM4/OPYC3 and HadCM2 experiments were obtained through the IPCC Data Distribution Centre. Michael Flechsig and Uta Fritsch of the Potsdam Institute for Climate Impact Research helped with the conversion of the global database on protected areas that was obtained from the World Conservation Monitoring Centre. The data set on the distribution of croplands was kindly provided by Navin Ramankutty of the University of Wisconsin-Madison.

The detailed and thoughtful comments of three anonymous reviewers are highly appreciated. They provided valuable suggestions for improving the paper. All remaining deficiencies are, however, the sole responsibility of the authors. Financial support for the ICLIPS project was provided by the German Federal Ministry of Education and Research (BMBF) under project number 01 LK 9605/0. The views presented here are those of the authors and do not necessarily represent the views of other ICLIPS partners or the project funders.

References

- Alcamo, J., Kreileman, E., Krol, M., Leemans, R., Bollen, J., van Minnen, J., Schaeffer, M., Toet, S., and de Vries, B.: 1998, 'Global modelling of environmental change: an overview of IMAGE 2.1', in J. Alcamo, R. Leemans, and E. Kreileman (eds.), *Global Change Scenarios of the 21st Century. Results from the IMAGE 2.1 Model*, Oxford: Pergamon, pp. 3–94.
- Bacher, A., Oberhuber, J.M., and Roeckner, E.: 1998, 'ENSO dynamics and seasonal cycle in the tropical Pacific as simulated by the ECHAM4/OPYC3 coupled general circulation model', *Climate Dynamics* **14**, 431–450.
- Batjes, N.H.: 1996, 'Development of a world data set of soil water retention properties using pedotransfer rules', *Geoderma* **71**, 31–52.
- Bergström, S.: 1995, 'The HBV model', in V. P. Singh (ed.), *Computer models of watershed hydrology*, Water Resources Publications, Highlands Ranch, CO, pp. 443–476.
- Bruckner, T., Petschel-Held, G., Toth, F.L., Füssel, H.-M., Helm, C., Leimbach, M., and Schellnhuber, H.-J.: 1999, 'Climate change decision-support and the tolerable windows approach', *Environmental Modeling and Assessment* **4**, 217–234.

- Bruckner, T., Petschel-Held, G., Leimbach, M., and Toth, F.L.: 2003a, 'Methodological aspects of the tolerable windows approach', *Climatic Change* (this issue).
- Bruckner, T., Hooss, G., Füssel, H.-M., and Hasselmann, K.: 2003b, 'Climate system modeling in the framework of the tolerable windows approach: The ICLIPS climate model', *Climatic Change* (this issue).
- Carter, T.R., Parry, M.L., Harasawa, H., and Nishioka, S.: 1994, *IPCC Technical Guidelines for Assessing Climate Change Impacts and Adaptations*, Part of the IPCC Special Report to the First Session of the Conference of the Parties to the UN Framework Convention on Climate Change, Department of Geography, University College London, London, UK.
- Dai, A., Meehl, G.A., Washington, W.M., Wigley, T.L., and Arblaster, J.M.: 2001, 'Ensemble Simulation of Twenty-First Century Climate Changes: Business-as-Usual versus CO₂ Stabilization', *Bulletin of the American Meteorological Society* **82**, 2377–2388.
- de Wit, C.T.: 1978, *Simulation of assimilation, respiration and transpiration of crops*, Simulation Monographs, PUDOC, Wageningen, The Netherlands.
- Döll, P., Kaspar, F., and Alcamo, J.: 1999, 'Computation of global water availability and water use at the scale of large drainage basins', *Mathematische Geologie* **4**, 111–118.
- FAO: 1981, 'Report on the agro-ecological zones project. Vol. 3: Methodology and results for South and Central America', World Soil Resources Report 48, Food and Agriculture Organization of the United Nations, Rome, Italy.
- FAO: 1988, 'FAO/UNESCO Soil Map of the World. Revised Legend', World Soil Resources Report 60, Food and Agriculture Organization of the United Nations, Rome, Italy.
- Foley, J.A., Prentice, I.C., Ramankutty, N., Levis, S., Pollard, D., Sitch, S., and Haxeltine, A.: 1996, 'An integrated biosphere model of land surface processes, terrestrial carbon balance, and vegetation dynamics', *Global Biogeochemical Cycles* **10**, 603–628.
- Füssel, H.-M. and van Minnen, J.G.: 2001, 'Climate impact response functions for the preservation of terrestrial ecosystems', *Integrated Assessment* **2**, 183–197.
- Grabs, W., de Couet, T., and Pauler, J.: 1996, 'Freshwater Fluxes from Continents into the World Oceans Based on Data of the Global Runoff Data Base', GRDC Report 10, Global Runoff Data Centre, Federal Institute of Hydrology, Koblenz, Germany.
- Henderson-Sellers, A.: 1996, 'Can we integrate climatic modelling and assessment?', *Environmental Modeling and Assessment* **1**, 59–70.
- Huntley, B., Berry, P.M., Cramer, W., and McDonald, A.P.: 1995, 'Modelling present and potential future ranges of some European higher plants using climate response surfaces', *Journal of Biogeography* **22**, 967–1001.
- IPCC (Intergovernmental Panel on Climate Change): 2000, *Special Report on Emissions Scenarios*, Cambridge University Press, Cambridge, UK.
- IUCN: 1998, *1997 United Nations List of Protected Areas*, World Conservation Union (IUCN), Gland, Switzerland.
- Johns, T.C., Carnell, R.E., Crossley, J.F., Gregory, J.M., Mitchell, J.F.B., Senior, C.A., Tett, S.F.B., and Wood, R.A.: 1997, 'The second Hadley Centre coupled ocean-atmosphere GCM: model description, spinup and validation', *Climate Dynamics* **13**, 103–134.
- Jones, T.H., Thompson, L.J., Lawton, J.H., Bezemer, T.M., Bardgett, R.D., Blackburn, T.M., Bruce, K.D., Cannon, P.F., Hall, G.S., Hartley, S.E., Howson, G., Jones, C.G., Kampichler, C., Kandeler, E., and Ritchie, D.A.: 1998, 'Impacts of rising atmospheric carbon dioxide on model terrestrial ecosystems', *Science* **280**, 441–443.
- Kirilenko, A.P. and Solomon, A.M.: 1998, 'Modeling dynamic vegetation response to rapid climate change using bioclimatic classification', *Climatic Change* **38**, 15–49.
- Klein Goldewijk, K., van Minnen, J.G., Kreileman, G.J.J., Vloedveld, M., and Leemans, R.: 1994, 'Simulating the carbon flux between the terrestrial environment and the atmosphere', *Water, Air, and Soil Pollution* **76**, 199–230.

- Leemans, R. and Hootsmans, R.: 1998, *Ecosystem vulnerability and climate protection goals*, Report No. 481508004, RIVM, Bilthoven, The Netherlands.
- Leemans, R. and van den Born, G.: 1994, 'Determining the potential global distribution of natural vegetation, crops and agricultural productivity', *Water, Air, and Soil Pollution* **76**, 133–162.
- Martin, P.H.: 1996, 'Will forest preserves protect temperate and boreal biodiversity from climate change?', *Forest Ecology and Management* **85**, 335–341.
- Mendelsohn, R., Schlesinger, M., and Williams, L.: 2000, 'Comparing impacts across climate models', *Integrated Assessment* **1**, 37–48.
- Mitchell, J.F.B., Johns, T.C., Eagles, M., Ingram, W.J., and Davis, R.A.: 1999, 'Towards the construction of climate change scenarios', *Climatic Change* **41**, 547–581.
- Mitchell, J.F.B., Johns, T.C., Ingram, W.J., and Lowe, J.A.: 2000, 'The effect of stabilising atmospheric carbon dioxide concentrations on global and regional climate change', *Geophysical Research Letters* **27**, 2977–2980.
- New, M., Hulme, M., and Jones, P.: 1999, 'Representing twentieth century space-time climate variability. Part I: Development of a 1961–1990 mean monthly terrestrial climatology', *Journal of Climate* **12**, 829–856.
- Nordhaus, W.D.: 1994, *Managing the Global Commons: The Economics of Climate Change*, MIT Press, Cambridge, MA.
- Nordhaus, W.D. and Boyer, J.: 2000, *Warming the World: Economic Models of Global Warming*, MIT Press, Cambridge, MA.
- Petschel-Held, G., Schellnhuber, H.-J., Bruckner, T., Toth, F.L., and Hasselmann, K.: 1999, 'The tolerable windows approach: theoretical and methodological foundations', *Climatic Change* **41**, 303–331.
- Prentice, I.C., Cramer, W., Harrison, S.P., Leemans, R., Monserud, R.A., and Solomon, A.M.: 1992, 'A global biome model based on plant physiology and dominance, soil properties and climate', *Journal of Biogeography* **19**, 117–134.
- Ramankutty, N. and Foley, J.: 1998, 'Characterizing patterns of global land use: an analysis of global croplands data', *Global Biogeochemical Cycles* **12**, 667–685.
- Robock, A., Turco, R.P., Harwell, M.A., Ackerman, T.P., Andressen, R., Chang, H.-S., and Sivakumar, M.V.K.: 1993, 'Use of GCM Output for Impact Analysis', *Climatic Change* **23**, 293–335.
- Roeckner, E., Arpe, K., Bengtsson, L., Christoph, M., Claussen, M., Dümenil, L., Esch, M., Giorgetta, M., Schlese, U., and Schulzweida, U.: 1996, *The Atmospheric General Circulation Model ECHAM-4: Model Description and Simulation of Present Day Climate*, Report No. 218, Max Planck Institute for Meteorology, Hamburg, Germany.
- Santer, B.D., Wigley, T.M.L., Schlesinger, M.E., and Mitchell, J.F.B.: 1990, *Developing Climate Scenarios from Equilibrium GCM Results*, Report No. 47, Max Planck Institute for Meteorology, Hamburg, Germany.
- Smith, J.B. and Pitts, G.J.: 1997, 'Regional climate change scenarios for vulnerability and adaptation assessments', *Climatic Change* **36**, 3–21.
- Tol, R.S.J.: 1996, 'The damage costs of climate change towards a dynamic representation', *Ecological Economics* **19**, 67–90.
- Tol, R.S.J.: 1999a, *New estimates of the damage costs of climate change, Part I: Benchmark estimates*, Working paper D99/01, Institute for Environmental Studies, Vrije Universiteit, Amsterdam, The Netherlands.
- Tol, R.S.J.: 1999b, *New estimates of the damage costs of climate change, Part II: Dynamic estimates*, Working paper D99/02, Institute for Environmental Studies, Vrije Universiteit, Amsterdam, The Netherlands.

- Toth, F.L.: 1996, 'Ecological damage functions', Paper presented at the Workshop on Climate Change: Integrating Science, Economics, and Policy, International Institute for Applied Systems Analysis, Laxenburg, Austria.
- Toth, F.L., Cramer, W., and Hizsnyik, E.: 2000, 'Climate impact response functions: an introduction', *Climatic Change* **46**, 225–246.
- Toth, F.L., Bruckner, T., Füssel, H.-M., Leimbach, M., and Petschel-Held, G.: 2003, 'Integrated assessment of long-term climate policies: Part 1 – Model presentation', *Climatic Change* (this issue).
- van Minnen, J.G., Alcamo, J., and Haupt, W.: 2000, 'Deriving and applying response surface diagrams for evaluating climate change impacts on crop production', *Climatic Change* **46**, 317–338.
- Villers-Ruíz, L. and Trejo-Vázquez, I.: 1998, 'Climate change on Mexican forests and natural protected areas', *Global Environmental Change* **8**, 141–157.
- von Storch, H.: 1995, 'Inconsistencies at the interface of climate impact studies and global climate research', *Meteorologische Zeitschrift* **4**, 72–80.